STIC-ILL

From: Canella, Karen
Sent: Thursday, May 22, 2003 9:50 PM
To: STIC-ILL
Subject: ill order 10/033,577

Art Unit 1642 Location 8E12(mail)

Telephone Number 308-8362

Application Number 10/033,577

1. Biochemistry, 2001 Apr 10, 40(4):4349-4358
2. PNAS, 1982, 79(9):2912-2916
3. Protein engineering, 1995, Vol. 8, suppl., page 123.

Proc. Natl. Acad. Sci. USA
Vol. 79, pp. 2912–2916, May 1982
Cell Biology

Receptor-mediated endocytosis of diphtheria toxin by cells in culture

(clustering/fluorescence/video intensification microscopy/clathrin-coated pits)

JAMES H. KEEN*, FREDERICK R. MAXFIELD†, M. CAROLYN HARDEGREE‡, AND WILLIAM H. HABIG‡

*Fels Research Institute, Temple University School of Medicine, Philadelphia, Pennsylvania 19140; †Department of Pharmacology, New York University Medical Center, New York, New York 10016; and ‡Food and Drug Administration, Bureau of Biologics, Bethesda, Maryland 20205

Communicated by Sidney Weinhouse, January 4, 1982

ABSTRACT The binding and uptake of fluorescently labeled diphtheria toxin by cells in culture has been examined by using epifluorescence video intensification microscopy. Rhodamine-labeled diphtheria toxin retained significant toxicity on bioassay and in cell culture and was tested for uptake by human WI-38 and mouse 3T3 fibroblasts grown in culture. When added to cells at 37°C, toxin was observed to become concentrated and internalized in discrete vesicles in both cell lines. The appearance of fluorescent clusters could be prevented by addition of excess unlabeled diphtheria toxin to the medium or by addition of ATP (which has been shown to block toxin binding to cells), indicating that the rhodamine-labeled toxin was binding to diphtheria toxin-specific cell surface binding sites. When the simultaneous uptake of rhodamine-labeled diphtheria toxin and fluorescein-labeled α_2-macroglobulin was monitored, the two proteins appeared in the same clusters indicating that the toxin undergoes receptor-mediated endocytosis. Despite the difference in susceptibility to diphtheria toxin of cells derived from sensitive (human) and resistant (mouse) tissues, the behavior of the rhodamine-labeled derivative in both cell lines was indistinguishable in terms of toxin required for formation of clusters or inhibition by unlabeled toxin or by ATP. These results demonstrate that diphtheria toxin-specific cell surface binding sites occur on both insensitive and sensitive cells and suggest that toxin is processed similarly by both cell types during its initial cell surface binding and internalization by this pathway. The possible involvement of this uptake system in the mechanism of action of diphtheria toxin in cells is discussed.

Extensive studies on the structure and mechanism of action of diphtheria toxin (DT) have resulted in a detailed understanding of the biochemical pathogenesis of the toxin (for review, see refs. 1 and 2). DT is synthesized by *Corynebacterium diphtheriae* lysogenic for the β^{tox+} phage and is secreted as a single polypeptide chain of M_r 62,000. The toxin can be nicked by proteases to yield A and B chains (M_r 21,000 and 41,000, respectively) that remain disulfide linked. The A chain catalyzes transfer of the ADP-ribose moiety of NAD to cytoplasmic elongation factor 2 (EF-2), resulting in the arrest of cellular protein synthesis. The B chain is catalytically inactive but appears to be responsible for cell surface binding. Although EF-2 from eukaryotic sources is highly conserved and isolated toxin A chain will ADP-ribosylate EF-2 proteins from all eukaryotic sources in cell-free extracts (3), rodents are relatively resistant to the actions of DT (1). This resistance is continued in cell lines derived from mouse or rat tissues.

Following earlier studies of the binding of DT to sensitive cells (4) and to membranes derived from both sensitive and insensitive cells (5), the existence of specific cell surface receptors on intact cells (6) has recently been documented. Incubation of toxin with cells at physiological temperature resulted in much of the toxin becoming inaccessible to external agents—suggesting entry into the cell. Finally, extensive degradation of toxin and inhibition of protein synthesis were observed (7).

The exact mechanisms by which toxin reaches the cell cytoplasm and the factors responsible for the phenomenon of resistance remain unknown. We have prepared a rhodamine-labeled derivative of diphtheria toxin (R-DT) that retained 25–50% of the biological activity of control preparations. Using this derivative and video intensification microscopy (8), we have found that toxin undergoes receptor-mediated endocytosis[§] (9): it is recognized by specific cell surface binding sites and is internalized in endocytic vesicles. Furthermore, this process occurs in both diphtheria toxin-sensitive and toxin-resistant cell lines. The implications of this uptake process for the toxicity of the protein are discussed.

MATERIALS AND METHODS

Swiss mouse 3T3 clone A and human WI-38 cells were grown as described (10). The WI-38 cells were used between passages 16 and 34 and a single lot of calf serum (GIBCO no. 12K3101) was used throughout these studies (11).

DT was obtained from John Robinson of Vanderbilt University. The preparation contained 20,000 minimum skin-reactive doses (MRD) per μg of protein (12) and was homogeneous on $NaDodSO_4$ gel electrophoresis. R-DT was prepared by reaction of DT with tetramethylrhodamine isothiocyanate; DT at 10 mg/ml in 0.05 M sodium borate (pH 9.2) was dialyzed for 24 hr at 4°C against 100 ml of 0.05 M sodium borate (pH 9.2) containing 2.0 mg of tetramethylrhodamine isothiocyanate (Cappel Laboratories, Cochranville, PA, lot no. 8612). The labeled protein was then dialyzed extensively against calcium- and magnesium-free Dulbecco's phosphate-buffered saline (P_i/NaCl) and then dialyzed overnight against P_i/NaCl supplemented with 1 M NaCl. Finally, the toxin was again dialyzed against P_i/NaCl. Fluorescein-labeled α_2-macroglobulin (F-α_2M) was prepared as described (13).

Bioactivity of the toxins was monitored in two ways. (*i*) Skin reactivity was assayed by (0.1 ml) intradermal injections of dilutions of the toxin in P_i/NaCl containing 0.2% gelatin into guinea pigs (12). The area of erythema was estimated as the product of two diameters measured at right angles to each other. (*ii*) *In vitro* protein synthesis assays were performed by using confluent monolayers of cells in 35-mm plastic dishes. The cells were washed and dilutions of DT or R-DT were added in 1.0

The publication costs of this article were defrayed in part by page charge payment. This article must therefore be hereby marked "*advertisement*" in accordance with 18 U. S. C. §1734 solely to indicate this fact.

Abbreviations: DT, diphtheria toxin; R-DT, rhodamine-labeled diphtheria toxin; α_2M, α_2-macroglobulin; F-α_2M, fluorescein-labeled α_2M; P_i/NaCl, phosphate-buffered saline; EF-2, elongation factor.

[§] The phrase "receptor-mediated endocytosis" is used to describe the process by which ligands are bound to specific cell surface binding sites, clustered and internalized into primary endocytic vesicles.

ml of complete medium. After 4 hr at 37°C, 0.5 μCi of L-[^{14}C(U)]leucine (339 mCi/mmol; 1 Ci = 3.7 × 10^{10} becquerels; Amersham) was added and incubation was continued for 3 hr. The cells were then washed three times with P_i/NaCl (containing calcium and magnesium) at 0°C and solubilized by addition of 1.0 ml of 0.1 M NaOH. The solution was acidified with 1.0 ml of 30% trichloroacetic acid; 75 μg of bovine serum albumin (Sigma) was added and the protein precipitate was washed with 1.0 ml of 10% trichloroacetic acid. Pellets were solubilized with 0.5 ml of 1 M NaOH and 0.5 ml of H_2O; 10 ml of ACS (aqueous counting scintillant, Amersham) was added and radioactivity in the samples was counted in an Intertechnique scintillation counter. Control incubations with cycloheximide (5 μg/ml, Sigma) were routinely performed.

For assay of R-DT interaction with cultured cells, cells were plated at 1.7 × 10^4 cells per cm^2 in 35-mm plastic dishes. The following day the dishes were washed three times with serum-free medium (37°C) and R-DT was added in 1.0 ml of serum-free medium containing 0.5% bovine serum albumin (37°C). After incubation for 15 or 30 min at 37°C, the dishes were washed three times with serum-free medium, then washed three times with P_i/NaCl, and finally were fixed by immersion in P_i/NaCl containing 3.7% formaldehyde. After several minutes, the dishes were rinsed in P_i/NaCl and mounted for microscopy.

Observation of the cells by phase-contrast and epi-fluorescence microscopy was performed as described (8) by using a Dage MTI model 65 silicon intensifier camera. For comparison, all images within each figure were obtained at constant manual settings of the camera gain, kV, and recorder video level controls.

Protein was assayed by the method of Lowry *et al.* (14) or that of Bradford (15). Bovine serum albumin or gamma globulin (Bio-Rad), respectively, was used for standards. All other chemicals were reagent grade or better.

RESULTS

Rhodamine-labeled derivatives of DT have been prepared to permit visualization of toxin interaction with cells in culture. Skin reactivity assays in guinea pigs revealed that increasing derivatization resulted in a progressive loss of biotoxicity (Fig. 1*A*). DT treated with 2.0 mg of tetramethylrhodamine isothiocyanate per 100 ml was found to retain ≈25% of the toxicity of the control; this preparation was used in all subsequent experiments. In short-term assays of inhibition of protein synthesis by sensitive (human WI-38) cells in culture, this R-DT preparation retained ≈50% of the activity of control preparations (Fig. 1*B*). In agreement with earlier studies (1, 16, 17), mouse (3T3) cells were resistant (Fig. 1*B*).

Toxin Uptake by Human Cells. To study the binding and uptake of toxin by human fibroblasts in culture, R-DT (65 nM) was incubated with WI-38 cells for 30 min. When rhodamine excitation–emission of the washed and fixed cells was monitored, a punctate pattern of fluorescence in the perinuclear region and extending throughout the cell was observed (Fig. 2*A*). Prominent autofluorescence in the WI-38 cells accounted for some of this signal as shown by examination of the same field by fluorescein excitation–emission (Fig. 2*B*). The autofluorescence component was generally diffuse or in large spots, was observed on untreated cells (not shown), and was characterized by a similar distribution and intensity with either the rhodamine or fluorescein filter set. Therefore, only that fluorescence on toxin-treated cells that was observed with the rhodamine but not with the fluorescein filter set was judged to reflect the presence of R-DT.

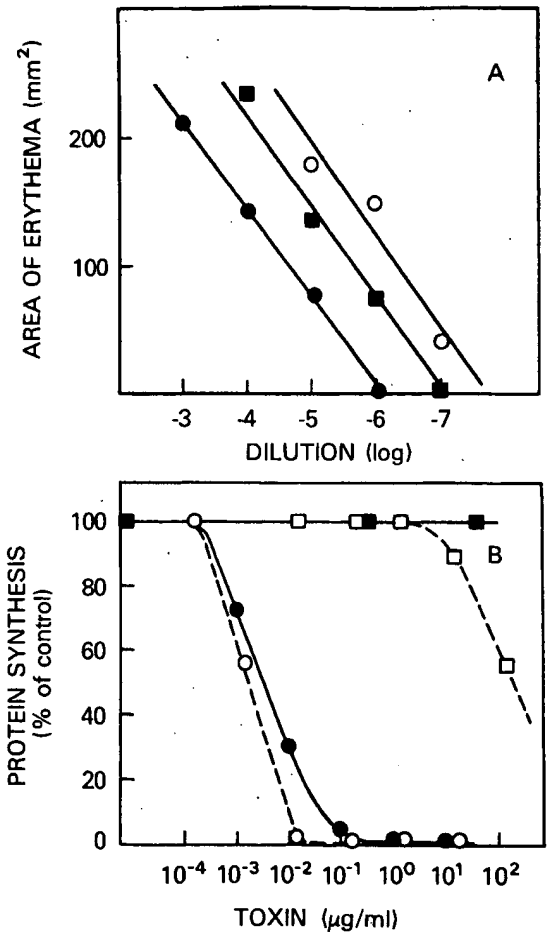

FIG. 1. Bioactivity of control DT and R-DT. (*A*) Guinea pig skin reactivity assay of control DT (○) and R-DT prepared with 2.0 (■) or 4.0 (●) mg of tetramethylrhodamine isothiocyanate (see *Materials and Methods*). All stock toxin concentrations were 3.0 mg/ml. (*B*) Effect of control DT (open symbols) and R-DT (closed symbols) on protein synthesis in human WI-38 (○, ●) or mouse 3T3 (□, ■) cells.

Although this punctate pattern of fluorescence could be recognized by using these concentrations, higher levels of R-DT (0.32 μM) increased the signal compared to the background autofluorescence and gave clearer patterns (Fig. 3). At these toxin concentrations, rhodamine-specific fluorescence is quite apparent (Fig. 3 *A–C*).

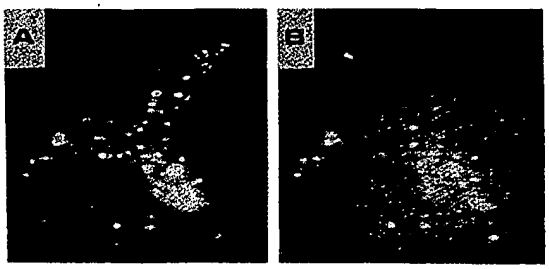

FIG. 2. Uptake of R-DT by human WI-38 cells. WI-38 cells were incubated in serum-free medium with R-DT (65 nM) for 30 min at 37°C. The cells were then observed by rhodamine (*A*) or fluorescein (*B*) epifluorescence. (×360.)

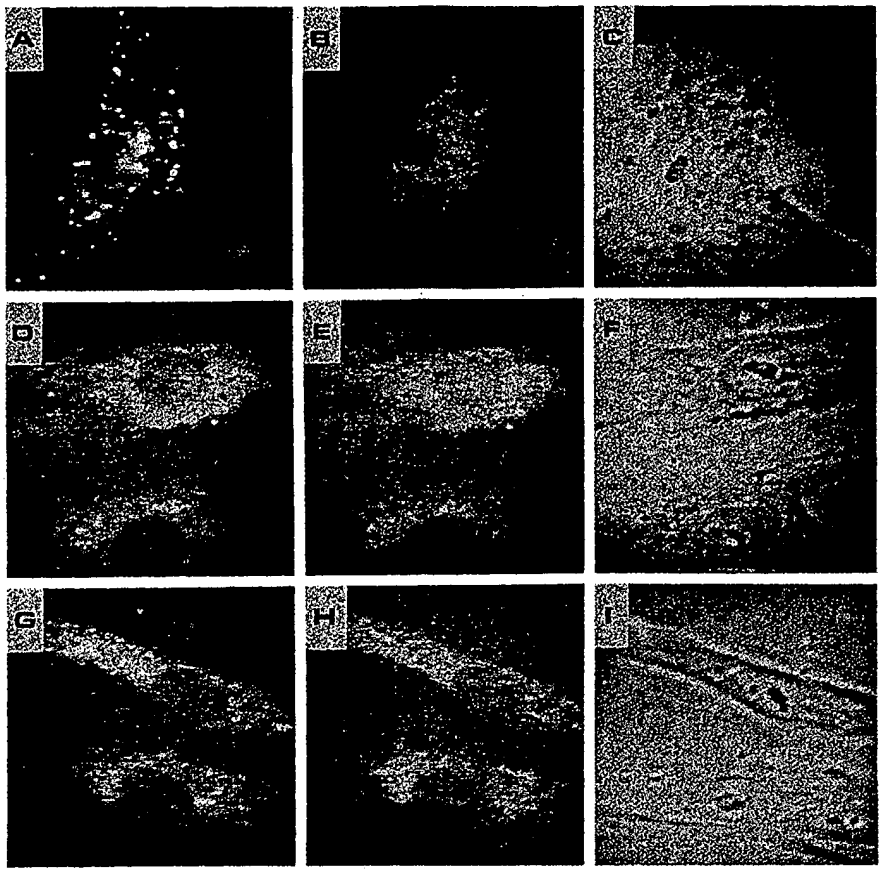

FIG. 3. Effect of unlabeled DT and ATP on the uptake of R-DT by WI-38 cells. WI-38 cells were incubated in serum-free medium with R-DT (0.32 μM) for 30 min at 37°C alone (*A–C*), in the presence of unlabeled toxin (39 μM) (*D–F*), or in the presence of ATP (5 mM) (*G–I*). In each experiment, the same field was observed by rhodamine (*A*, *D*, and *G*) or fluorescein (*B*, *E*, and *H*) epi-fluorescence or by phase-contrast optics (*C*, *F*, and *I*). (×370.)

The specificity of this pattern was investigated in two additional ways. Incubation of WI-38 cells with R-DT in the presence of a 120-fold excess of unlabeled toxin blocked the formation of all rhodamine-specific fluorescent clusters (Fig. 3 *D–F*), indicating that binding of the rhodamine-labeled toxin is saturable and is competitively inhibited by the native toxin. Nucleotides—in particular ATP and other triphosphates—have been shown to block DT binding to cell surface receptors and to prevent the expression of biotoxicity (6, 18). When ATP (5 mM) was included with R-DT in the incubation medium of WI-38 cells, formation of the fluorescent pattern described above was blocked (Fig. 3 *G–I*). Substantial effect was also observed at lower ATP concentrations (0.5–1.0 mM), although CTP (up to 3 mM) had much less effect (not shown), in agreement with earlier findings (18). Nucleotides were entirely without effect on the clustering of F-α_2M (not shown). These results and the competition by unlabeled toxin indicate that the R-DT is binding to specific cell surface sites and that these sites have properties consistent with those observed for toxin receptors in other systems (6).¶

Toxin Uptake by Mouse Cells. Rats and mice (and cultured cells derived from rodent tissues) are much less sensitive to the actions of DT than their nonrodent counterparts (16, 17). However, when inhibition of protein synthesis is measured in cell-free extracts, all eukaryotic preparations are uniformly susceptible to the action of the toxin (3). Therefore, it was of particular interest to ask whether R-DT would interact specifically with resistant rodent cells. Incubation of R-DT with Swiss mouse 3T3 fibroblasts—under conditions similar to those employed with human WI-38 fibroblasts—resulted in the formation of fluorescent clusters indistinguishable in appearance from those observed with the human cells (Fig. 4 *A* and *B*). The appearance of these clusters was blocked by simultaneous incubation with excess unlabeled toxin (Fig. 4 *C* and *D*) and, as with the human cells, ATP (5 mM) also prevented the formation of the R-DT clusters on the mouse fibroblasts (Fig. 4 *E* and *F*). Thus, these resistant cells also possess specific toxin binding sites.

Co-Localization of R-DT and F-α_2M. To specifically determine whether the fluorescent clusters of R-DT observed on 3T3 cells were likely to have been formed in clathrin-coated pits, we studied the simultaneous uptake of R-DT with F-α_2M. The distribution of R-DT in (and on) a cell after a 30-min incubation is shown in Fig. 5*A* and the localization of F-α_2M in the same field is shown in Fig. 5*B*. Superimposition of positive transparencies of *A* and *B* reveals that most of the spots are coincident in both fields (Fig. 5*C*), demonstrating that F-α_2M and R-DT are present in the same structures. Coincidence of the fluorescence due to random overlap is rare as shown in Fig. 5*D*; here one of the transparencies has been shifted (about 1 mm in the scale of the figure) and very few fluorescent spots are observed.

¶ Because the R-DT has not been physically isolated, we cannot rule out the formal possibility that it is being processed differently from the unlabeled material in some way that we do not detect.

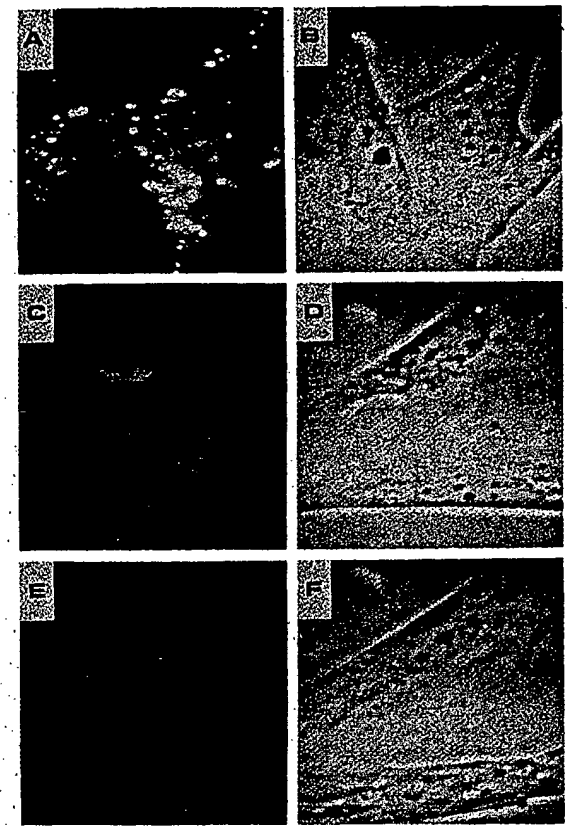

FIG. 4. Uptake of R-DT by Swiss mouse 3T3 cells. Cells were incubated in serum-free medium for 30 min at 37°C with R-DT (0.48 μM) alone (*A* and *B*) or in the presence of unlabeled toxin (39 μM) (*C* and *D*) or ATP (5 mM) (*E* and *F*). The same field was then observed by rhodamine epi-fluorescence (*A*, *C*, and *E*) or by phase-contrast optics (*B*, *D*, and *F*). No image was observed by fluorescein epi-fluorescence. (×360.)

R-DT and F-α_2M fluorescence was also coincident when a 15-min incubation was performed (data not shown). Electron microscopic studies with 3T3 cells have shown that α_2-macroglobulin (α_2M) is internalized through clathrin-coated pits (19) and within the first 30 min (13, 20) is localized predominantly in primary endocytic vesicles (receptosomes). Thus, these results suggest that R-DT is also being processed in this manner by mouse cells.

DISCUSSION

Although the broad outline of toxin–cell interactions is clear, the details of the process by which active toxin traverses the membrane and reaches the cell cytoplasm remain unclear. Furthermore, the nature of the differences responsible for sensitivity and resistance is unknown—despite the equal susceptibility of EF-2 from all eukaryotic sources to toxin *in vitro*. The results reported here demonstrate that DT undergoes internalization by receptor-mediated endocytosis as do serum proteins, peptide hormones, and viruses (9, 21). In addition, we demonstrate that this uptake pathway operates in both toxin-sensitive and toxin-resistant cells.

The formation of fluorescent R-DT clusters on cells could be blocked by an excess of unlabeled toxin, indicating the involvement of specific and saturable binding sites. Nucleotides have been shown both to block the expression of toxicity in sensitive cells and to inhibit DT binding to specific high-affinity sites on

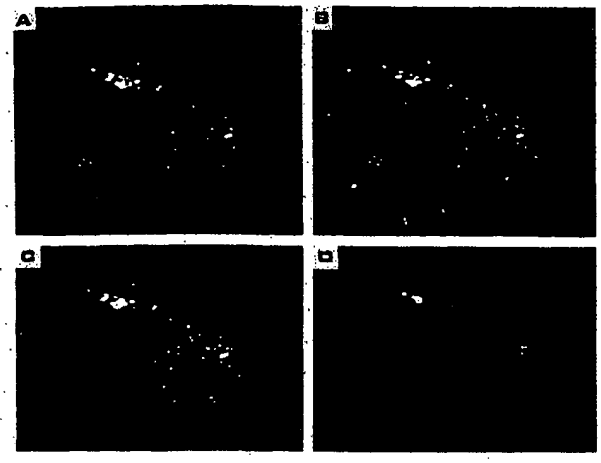

FIG. 5. Simultaneous uptake of R-DT and F-α_2M by Swiss mouse 3T3 cells. Cells were incubated with R-DT (0.32 μM) and F-α_2M (50 μg/ml) for 30 min at 37°C. The same field was then observed by rhodamine (*A*) and fluorescein (*B*) epi-fluorescence. Alignment of positive transparencies of *A* and *B* resulted in *C*, whereas slight misalignment (about 1 mm) produced *D*. (×340.)

cells or on isolated membranes (5, 18). ATP entirely blocked the formation of fluorescent clusters of R-DT on both sensitive and resistant cells whereas CTP was ineffective, in agreement with previously published studies on ^{125}I-labeled DT binding to cells (18). The coincidence of R-DT and F-α_2M fluorescence at both 15 and 30 min indicates that both proteins are present in the same endocytic vesicle at these times and suggests that DT—like α_2M (10, 19)—is internalized after clustering in clathrin-coated pit regions of the plasma membrane. Recently, ultrastructural studies with another protein toxin, *Pseudomonas* exotoxin A, revealed that it was bound and clustered in coated pits on mouse LM cells (22).

The toxin concentrations ($\approx 10^{-7}$ M) used in this study are substantially greater than LD_{50} values ($\approx 10^{-10}$ M) (6); this raises a question concerning the relevance of our observations to the toxic process in cells. In toxicity studies, a small number of molecules [possibly only one (23)] enters the cytoplasm and acts catalytically for hours. Higher toxin concentrations were required to study early events in the toxic process—the cell surface binding and internalization that occur during the first 30 min. However, it should be noted that the toxin concentrations used approximate toxin–receptor dissociation constants (10^{-9}–10^{-7} M) that have been measured with intact cells (6, 24) or isolated membranes (5).

There are several arguments in support of the hypothesis that the process of receptor-mediated endocytosis that we have observed is a physiologically relevant pathway for toxin entry. The binding of R-DT is specific and saturable, and the appearance of R-DT in endocytic vesicles can be inhibited by nucleotides that block DT toxicity. The rate at which ligands such as α_2M are cleared from the cell surface by receptor-mediated endocytosis (9) is similar to the rate at which ^{125}I-labeled DT is internalized (7). Toxin-specific antibody and concanavalin A have been shown to inhibit the internalization of ^{125}I-labeled DT: both also block the cytotoxic effect (7).

Rapid degradation of internalized toxin, characteristic of lysosomal involvement, has also been documented (7). Chloroquine (25) and other lysosomotropic agents (26–28) that prevent this lysosomal degradation of toxin also block its toxic effect. Finally, reduction of the extracellular pH to a level approximating that in the lysosome results in rapid intoxication of sen-

sitive cells (27, 29) and in association of toxin with synthetic membranes (30). These observations are consistent with passage across the limiting membrane and entry of toxin into the cytoplasm only after delivery to an acidic environment. In fact, Tycko and Maxfield (31) have recently shown that primary endocytic vesicles containing α_2M, in which we also find R-DT, have a pH of 5.0 ± 0.2 (±SEM). Thus, the receptor-mediated endocytosis of R-DT that we have observed, whereby ligands are internalized into primary endocytic vesicles and delivered to lysosomes (9, 13), has many of the properties of the toxic pathway. Nonetheless, we cannot exclude the possibility that additional entry pathways—which we were unable to detect—share these properties and contribute to or are entirely responsible for toxicity.

We have observed receptor-mediated endocytosis of DT in resistant mouse fibroblasts as well as in sensitive cells. These experiments confirm the earlier observations of Chang and Neville (5) that DT-specific binding sites exist on resistant cells. Sandvig and Olsnes (29) noted that acidification of the extracellular medium did not result in rapid intoxication of resistant mouse cells. This observation and the results reported here suggest that post-internalization factors may be responsible for the resistance manifested by rodent cells—e.g., retention of toxin in the lysosome despite the acidic environment (29) or the absence of a gene product responsible for translocation into the cytoplasm (32). Alternatively, the endocytosis pathway may be unrelated to the toxic process. The present data do not allow us to definitively distinguish among these possibilities and further studies are clearly indicated.

We are grateful to Charles O. Boyd and Gwen Koths for assistance in preparing the figures and to Sherry Battaglia for typing the manuscript. This study was supported by National Institutes of Health research Grants GM 28526 (J.H.K.) and CA 12227 (to the Fels Research Institute).

1. Collier, R. J. (1975) *Bacteriol. Rev.* 39, 54–85.
2. Pappenheimer, A. M., Jr. (1977) *Annu. Rev. Biochem.* 46, 69–94.
3. Johnson, W., Kuchler, R. J. & Solotorovsky, M. (1968) *Bacteriology* 96, 1089–1098.
4. Boquet, P. & Pappenheimer, A. M., Jr. (1976) *J. Biol. Chem.* 251, 5770–5778.
5. Chang, T.-M. & Neville, D. M., Jr. (1978) *J. Biol. Chem.* 253, 6866–6871.
6. Middlebrook, J. L., Dorland, R. B. & Leppla, S. H. (1978) *J. Biol. Chem.* 253, 7325–7330.
7. Dorland, R. B., Middlebrook, J. L. & Leppla, S. H. (1979) *J. Biol. Chem.* 254, 11337–11342.
8. Willingham, M. C. & Pastan, I. (1978) *Cell* 13, 501–507.
9. Goldstein, J. L., Anderson, R. G. W. & Brown, M. S. (1979) *Nature (London)* 279, 679–685.
10. Maxfield, F. R., Schlessinger, J., Shechter, Y., Pastan, I. & Willingham, M. C. (1978) *Cell* 14, 805–810.
11. Middlebrook, J. L. & Dorland, R. B. (1977) *Can. J. Microbiol.* 23, 175–182.
12. Barile, M. F., Kolb, R. W. & Pittman, M. (1971) *Infect. Immun.* 4, 295–306.
13. Willingham, M. C., Maxfield, F. R. & Pastan, I. (1980) *J. Histochem. Cytochem.* 28, 818–823.
14. Lowry, O. H., Rosebrough, N. J., Farr, A. L. & Randall, R. J. (1951) *J. Biol. Chem.* 193, 265–275.
15. Bradford, M. M. (1976) *Anal. Biochem.* 72, 248–254.
16. Gabliks, J. & Solotorovsky, M. (1962) *J. Immunol.* 88, 505–512.
17. Bonventre, P. F. & Imhoff, J. G. (1968) *J. Exp. Med.* 126, 1079–1086.
18. Middlebrook, J. L. & Dorland, R. B. (1979) *Can. J. Microbiol.* 25, 285–290.
19. Willingham, M. C., Maxfield, F. R. & Pastan, I. (1979) *J. Cell Biol.* 82, 614–625.
20. Willingham, M. C. & Pastan, I. (1980) *Cell* 21, 67–77.
21. Helenius, A., Kartenbeck, J., Simons, K. & Fries, E. (1980) *J. Cell Biol.* 84, 404–420.
22. Fitzgerald, D., Morris, R. E. & Saelinger, C. B. (1980) *Cell* 21, 867–873.
23. Yamaizumi, M., Mekada, E., Uchida, T. & Okada, Y. (1978) *Cell* 15, 245–250.
24. Uchida, T., Pappenheimer, A. M., Jr. & Harper, A. (1973) *J. Biol. Chem.* 248, 3845–3850.
25. Leppla, S. H., Dorland, R. B. & Middlebrook, J. L. (1980) *J. Biol. Chem.* 255, 2247–2250.
26. Kim, K. & Groman, N. B. (1965) *J. Bacteriol.* 90, 1552–1556.
27. Draper, R. & Simon, M. I. (1980) *J. Cell Biol.* 87, 849–854.
28. Mekada, E., Uchida, T. & Okada, Y. (1981) *J. Biol. Chem.* 256, 1225–1228.
29. Sandvig, K. & Olsnes, S. (1980) *J. Cell Biol.* 87, 828–832.
30. Donovan, J. J., Simon, M. I., Draper, R. K. & Montal, M. (1981) *Proc. Natl. Acad. Sci. USA* 78, 172–176.
31. Tycko, B. & Maxfield, F. R. (1982) *Cell*, in press.
32. Creagan, R. P., Chen, S. & Ruddle, F. H. (1975) *Proc. Natl. Acad. Sci. USA* 72, 2237–2241.

STIC-ILL

NPL

From: Canella, Karen
Sent: Thursday, May 22, 2003 9:50 PM
To: STIC-ILL
Subject: ill order 10/033,577

Art Unit 1642 Location 8E12(mail)

Telephone Number 308-8362

Application Number 10/033,577 #14

1. Biochemistry, 2001 Apr 10, 40(4):4349-4358
2. PNAS, 1982, 79(9):2912-2916
3. Protein engineering, 1995, Vol. 8, suppl., page 123.

Ability of the Tat Basic Domain and VP22 To Mediate Cell Binding, but Not Membrane Translocation of the Diphtheria Toxin A-Fragment†

Pål Ø. Falnes,*,‡ Jørgen Wesche,§ and Sjur Olsnes

Institute for Cancer Research, The Norwegian Radium Hospital, Montebello, 0310 Oslo, Norway

Received October 23, 2000; Revised Manuscript Received January 3, 2001

ABSTRACT: A number of proteins are able to enter cells from the extracellular environment, including protein toxins, growth factors, viral proteins, homeoproteins, and others. Many such translocating proteins, or parts of them, appear to be able to carry with them cargo into the cell, and a basic sequence from the HIV-1 Tat protein has been reported to provide intracellular delivery of several fused proteins. For evaluating the efficiency of translocation to the cytosol, this TAT-peptide was fused to the diphtheria toxin A-fragment (dtA), an extremely potent inhibitor of protein synthesis which normally is delivered efficiently to the cytosol by the toxin B-fragment.The fusion of the TAT-peptide to dtA converted the protein to a heparin-binding protein that bound avidly to the cell surface. However, no cytotoxicity of this protein was detected, indicating that the TAT-peptide is unable to efficiently deliver enzymatically active dtA to the cytosol. Interestingly, the fused TAT-peptide potentiated the binding and cytotoxic effect of the corresponding holotoxin. We made a fusion protein between VP22, another membrane-permeant protein, and dtA, and also in this case we detected association with cells in the absence of a cytotoxic effect. The data indicate that transport of dtA into the cell by the TAT-peptide and VP22 is inefficient.

The plasma membrane of cells is generally impermeable to proteins and peptides. While the cell has developed a complex system for exporting secretory proteins, little transfer of proteins is thought to occur in the opposite direction, i.e., from the extracellular environment to the cytosol. However, some proteins represent an exception to this rule, and are able to enter the cytosol when added extracellularly. These include plant and bacterial toxins (*1*), growth factors (*2*), homeoproteins (*3*), and some viral proteins (*4*−*6*).

Plant and bacterial toxins acting on intracellular targets commonly consist of two moieties, denoted A and B, where the B moiety mediates binding of the toxin to cell-surface receptors and often plays a role in mediating the transfer of the A moiety across cellular membranes (reviewed in ref *1*). The A moiety is an enzyme which enters the cytosol and modifies a target, leading to cell death or having detrimental effects on cellular physiology with serious consequences for the whole organism. Diphtheria toxin is synthesized as one polypeptide of 58 kDa by *Corynebacterium diphtheriae* (*7*), and treatment of the toxin with trypsin-like proteases converts it into its active form, which consists of two fragments, A (21 kDa) and B (37 kDa) (*8*), linked by a disulfide bond (*9*). Toxin entry into cells is initiated by binding of the B-fragment to the toxin receptor (*10*) which is identical to the uncleaved precursor of heparin-binding epidermal growth factor-like growth factor (*11*). Receptor binding is followed by endocytosis, and the low pH in endosomes induces unfolding of the toxin molecule (*12*, *13*), leading to insertion of the B-fragment into the endosomal membrane and translocation of the A-fragment (dtA)[1] to the cytosol. Also, if cell-surface-bound toxin is exposed to a buffer of acidic pH, thereby mimicking the conditions in the endosome, the translocation process is induced at the level of the plasma membrane (*14*, *15*). This translocation process is very efficient: 50% of the bound toxin molecules are typically translocated to the cytosol (*16*, *17*). Once in the cytosol, the A-fragment causes inhibition of cellular protein synthesis through catalyzing the ADP-ribosylation of elongation factor 2, and the presence of a single A-fragment in the cytosol of a cell appears to be sufficient to completely block protein synthesis and kill the cell (*17*, *18*).

During the past decade, it has been reported that peptide sequences derived from proteins with membrane translocating ability are able to function as vehicles for the transport of other proteins into the cell. HIV-1 encodes the transactivating protein Tat, which is essential for the expression of viral genes, and exogenously added Tat has been shown to enter cells (*5*, *6*). A Tat-derived, basic sequence of 11 amino acids has been claimed to confer membrane translocating activity to several proteins of sizes up to 120 kDa (*19*, *20*). Similarly, the tegument protein VP22 from herpes simplex virus type 1 has also been reported to mediate transfer of heterologous proteins into cells (*4*, *21*). A positively charged, 16 residue peptide derived from the third

† This work was supported by the Norwegian Cancer Society, the Bruun Fund, the Blix Fund, and the Jahre Foundation.

* To whom correspondence should be addressed. Email: pfalnes@labmed.uio.no. Phone: 47-23074063. Fax: 47-23074061.

‡ Holder of a Career Investigator Fellowship from the Norwegian Cancer Society.

§ Fellow of the Norwegian Cancer Society.

[1] Abbreviations: aFGF, acidic fibroblast growth factor; dtA, diphtheria toxin A-fragment; dtB, diphtheria toxin B-fragment; ER, endoplasmic reticulum; FCS, fetal calf serum; HIV-1, human immunodeficiency virus type 1; MES, 2-(*N*-morpholino)ethanesulfonic acid; NEM, *N*-ethylmaleimide; PBS, phosphate-buffered saline; PAGE, polyacrylamide gel electrophoresis; PMSF, phenylmethylsulfonyl fluoride; TCA, trichloroacetic acid.

10.1021/bi0024431 CCC: $20.00
Published on Web 03/15/2001

helix of the homeodomain of the Antennapedia protein has been reported to mediate transport into cells of peptides of up to 100 residues in size (*22*). Interestingly, all these sequences are highly positively charged, and they have been reported to bind to heparin (*22*−*26*), suggesting that they are capable of binding to cell-surface heparans, similar to many growth factors. The transport phenomena mediated by these peptides appear to share several features; i.e., it is claimed that binding to cell-surface receptors is not involved, and that translocation occurs even at 4 °C, arguing against the involvement of conventional endocytosis.

The transport into cells of heterologous proteins consisting of the alleged membrane-permeant sequences fused to biologically active cargo molecules has mainly been studied by immunofluorescence microscopy, and by assaying for an intracellular biological activity displayed by the cargo. When using immunofluorescence microscopy, it may be difficult to distinguish between free cytosolic protein and material associated with membrane-bound organelles. Thus, it still remains unclear whether the translocation of such proteins to the cytosol is an efficient process, or whether only a minute fraction of the cell-associated protein actually can reach the cytosol or another desired location, e.g., the nucleus. Also, virtually nothing is known regarding the mechanism of cellular targeting or membrane penetration by such proteins.

The translocation of dtA into cells by the toxin's own translocation machinery, dtB, is an efficient process that has been well characterized, and the translocation of only a few molecules of dtA per cell is readily detected in cytotoxicity experiments. We were therefore interested in comparing the efficiency of delivery of dtA in the context of the holotoxin, with that provided by the TAT-peptide and VP22, two membrane-permeant sequences that have been reported to be able to deliver large proteins into cells.

EXPERIMENTAL PROCEDURES

Buffers, Media, and Reagents. [^{3}H]Leucine and [^{35}S]-methionine were from NEN (Boston, MA). Crude diphtheria toxin from Connaught Laboratories (Willowdale, Canada) was purified as described (*27*). Dialysis buffer consisted of 140 mM NaCl, 20 mM HEPES, and 2 mM $CaCl_2$, adjusted to pH 7.0 with NaOH. HEPES medium is bicarbonate-free Eagle's minimal essential medium buffered with 20 mM HEPES and adjusted with NaOH to pH 7.4. MES−gluconate buffer is 140 mM NaCl, 5 mM sodium gluconate, 20 mM MES, adjusted with Tris to pH 4.8 or pH 7.0. Lysis buffer consisted of 0.1 M NaCl, 20 mM NaH_2PO_4, 10 mM EDTA, 1% Triton X-100, 1 mM PMSF, 1 mM NEM, pH 7.4. Phosphate-buffered saline (PBS) is 140 mM NaCl, 10 mM NaH_2PO_4, pH 7.4.

Cell Cultures. Vero cells were maintained and propagated under standard conditions (5% CO_2 in Eagle's minimal essential medium containing 5% FCS). For toxicity and binding/translocation experiments, the cells were seeded into 24 well Costar plates on the day preceding the experiments at densities of 5×10^4 and 1×10^5 cells per well, respectively.

Plasmid Construction. The primer AATTAACCCTCACTAAAGCCGCCATGGGCTACGGTAGGAA GAAGCGTCGTCAAAGGCGTAGGGGCGCTGATGATGTTGTTGATTCTTCT, which contains (in the following order) a T3 promoter, an *Nco*I site, and sequences encoding the TAT-peptide and the nine N-terminal amino acids of the diphtheria toxin A-fragment, was used as a forward primer in a PCR reaction where plasmid pkD-52 (encoding the wild-type A-fragment) (*28*) was used as template, and a primer annealing downstream of the toxin gene was used as reverse primer. We first tried to use the PCR product directly as template for in vitro transcription with T3 RNA polymerase, but these attempts were not successful. The PCR-product was therefore cleaved with *Nco*I and *Acc*I, and cloned into the corresponding sites of pKD-52, generating the plasmid encoding TAT-dtA. The sequence of the region generated by PCR was verified by dideoxy sequencing.

The plasmid encoding VP22-dtA was constructed by fusing the cDNA coding for the diphtheria toxin A-fragment to the 3′ end of VP22 in the pVP22/myc-His plasmid from Invitrogen (Groningen, The Netherlands). A sequence encoding a glycine linker was inserted between the VP22 and dtA genes to ensure flexibility between the two domains (see Figure 7A).

In Vitro Transcription and Translation. Plasmid DNA was linearized downstream of the encoded gene, and transcription was carried out in a 20 μL reaction mixture with T3 or T7 RNA polymerase as described (*29*). The mRNA was precipitated with ethanol and dissolved in 10 μL of H_2O containing 10 mM DTT and 0.1 unit/μL RNasin (Promega, Madison, WI). The translation was performed for 1 h at 30 °C in micrococcal nuclease treated rabbit reticulocyte lysate (Promega, Madison, WI) containing 1 μM [^{35}S]methionine and 25 μM of each of the other 19 amino acids, and 5 μL of the dissolved mRNA was used per 100 μL of lysate. When unlabeled A- and B-fragments were prepared, radiolabeled methionine was replaced by 25 μM unlabeled methionine.

In Vitro Reconstitution of Active Toxin. When A-fragment and B-fragment are mixed under reducing conditions, and the reducing agent is subsequently removed by dialysis, active heterodimeric toxin will form quantitatively (*30*). [^{35}S]-Methionine-labeled A-fragment and unlabeled B-fragment were made separately by in vitro transcription and translation, the translation mixtures were mixed together in a 1:1 ratio, and formation of the interfragment disulfide bond was facilitated by overnight dialysis against dialysis buffer. The concentrations of the different toxins were estimated by SDS−PAGE and phosphorimaging. Typically, the concentration of reassociated holotoxin in the dialyzed translation mixture was 2 nM. To avoid cellular incorporation of residual [^{35}S]methionine present in dialyzed translation mixtures, 1 mM of unlabeled methionine was added before the mixture was incubated with cells. In some cases, unlabeled toxin was prepared (for the purpose of being able to use higher toxin concentrations in the toxicity experiments, as in Figure 2). The toxin concentration was then estimated by calculating the concentration in a [^{35}S]methionine-labeled aliquot prepared in parallel, as previously described (*30*).

Cytotoxicity Measurements. Overnight toxicity (Figures 2 and 7B): Vero cells were incubated for 16 h in growth medium at 37 °C with increasing amounts of in vitro translated, unlabeled toxin. The cells were washed in leucine-free HEPES medium for 5 min, followed by incubation for 30 min at 37 °C in leucine-free HEPES medium with 4 μCi/mL [^{3}H]leucine. Cellular proteins were then precipitated in the tissue culture well with 5% TCA for 10 min at room

temperature, washed once with TCA, and, finally, dissolved in 0.1 M KOH. The radioactivity incorporated into cellular proteins was measured by scintillation counting. Low-pH-induced cytotoxicity (Figure 6A): Vero cells were incubated for 1 h at 4 °C with increasing amounts of [^{35}S]methionine-labeled, in vitro translated toxin, and then washed 3 times in dialysis buffer to remove unbound toxin. The cells were then incubated for 5 min at 37 °C in MES−gluconate buffer, pH 4.8, and subsequently incubated for 16 h in growth medium in the presence of 10 μM monensin to prevent translocation from endosomes. Finally, the cells were washed in leucine-free HEPES medium, and the incorporation of [^{3}H]-leucine was measured as for the overnight toxicity experiment.

Cytotoxic effect of brief exposure to toxin (Figure 6B): Vero cells were incubated for 30 min in growth medium at 37 °C with increasing amounts of [^{35}S]methionine-labeled, in vitro translated toxin, and then washed 4 times in dialysis buffer to remove unbound toxin. The cells were then incubated for 16 h in growth medium and then washed in leucine-free HEPES medium, and the incorporation of [^{3}H]leucine was measured as for the overnight toxicity experiment.

Binding of Toxin to Cells. Vero cells were incubated with increasing concentrations of [^{35}S]methionine-labeled toxin in HEPES medium for 1 h at 4 °C or for 30 min at 37 °C, washed 4 times in dialysis buffer, and lysed for 10 min on ice in lysis buffer. The cell lysate was transferred to an Eppendorf tube, and cellular proteins were precipitated for 30 min on ice with 5% TCA. After centrifugation, the TCA pellet was washed twice in ether and subjected to SDS−PAGE and fluorography or phosphorimaging. The amount of [^{35}S]methionine-labeled protein present in the bands in the gels was measured by phosphorimaging (Figure 4A,B), or in some cases, when the signals were weak (Figure 4C), by densitometric scanning of the film after fluorography.

Binding of Toxin to Heparin−Sepharose. A 0.5 μL sample of dialyzed translation mixture containing [^{35}S]methionine-labeled toxin was incubated under rotation for 1 h at 4 °C with 15 μL of heparin−Sepharose (prewashed with PBS) in a total volume of 400 μL of PBS with 0.1% Triton X-100 in an Eppendorf tube. The heparin−Sepharose was collected by centrifugation and the supernatant discarded. After three washes of the heparin−Sepharose with 1 mL of PBS with 0.1% Triton X-100, the proteins were eluted by heating to 95 °C in reducing SDS−PAGE sample buffer, and subsequently analyzed by SDS−PAGE and fluorography.

Pronase Protection Experiments. Vero cells were incubated with [^{35}S]methionine-labeled, reconstituted toxin (0.5 nM) in the presence of 10 μM monensin for 20 min at 25 °C, and then washed 3 times with dialysis buffer to remove unbound toxin. After a 2 min exposure to MES−gluconate buffer, pH 4.8, at 37 °C, the cells were incubated for 10 min at 37 °C with 5 mg/mL Pronase E in HEPES medium containing 10 μM monensin. The cells, which then were detached from the plastic, were transferred to an Eppendorf tube, and pelleted by centrifugation. After washing with HEPES medium containing 1 mM NEM and 1 mM PMSF, the cells were lysed for 10 min in lysis buffer on ice, and nuclei were removed by centrifugation. Cellular protein was precipitated with 5% TCA for 30 min on ice, and pelleted by centrifugation. The pellet was washed with ether and subjected to SDS−PAGE under nonreducing conditions.

Measurement of ADP-Ribosylating Activity. The experiment was performed essentially as described earlier (*31*). We measured the ability of dtA and VP22-dtA to incorporate ADP-ribose from [*adenylate*-^{32}P]NAD into EF-2 by removing aliquots of the reaction mixture after different times of incubation at 25 °C. Reticulocyte lysate was used as a source of EF-2. The samples were analyzed immediately by SDS−PAGE. Phosphorimaging was used to estimate the relative amount of radioactivity incorporated into EF-2 after different times of incubation, and the enzymatic activity was calculated.

RESULTS

Construction of dtA with an N-Terminal TAT-Peptide. By a PCR-based approach, we constructed a plasmid, denoted TAT-dtA, encoding the diphtheria toxin A-fragment with the TAT-peptide fused to its N-terminus. Radiolabeled protein was generated by in vitro transcription with T3 RNA polymerase, followed by translation in a reticulocyte lysate in the presence of [^{35}S]methionine. When dtA is produced by in vitro translation and subsequently mixed with in vitro translated B-fragment (dtB), removal of reducing agents by dialysis leads to quantitative formation of the holotoxin (dtA+dtB), due to interfragment disulfide bond formation (Figure 1A). We first tested whether radiolabeled TAT-dtA was capable of forming an interfragment disulfide bond upon mixing with unlabeled dtB. The results (Figure 1B) showed that this was indeed the case. The A-fragment (dtA or TAT-dtA) was in excess relative to dtB, and only a fraction of it is therefore converted to holotoxin.

Measurement of Cytotoxicity upon Overnight Incubation with Toxin. Upon binding of the holotoxin (dtA+dtB) to cells, dtA enters the cytosol, leading to inhibition of cellular protein synthesis. It has been reported that an attached TAT-peptide can mediate the translocation of proteins into cells, causing measurable biological effects (*32*, *33*). We were therefore interested in testing whether TAT-dtA would inhibit cellular protein synthesis, and we incubated Vero cells with increasing concentrations of this protein. As with dtA alone, we could not detect any cytotoxic effect of TAT-dtA (Figure 2). On the other hand, the corresponding holotoxins, dtA+dtB and TAT-dtA+dtB, were both highly cytotoxic, with similar potency. Thus, with the relatively modest amounts of protein obtained by in vitro translation, we could not detect any translocation of TAT-dtA to the cytosol. The data therefore indicate that the TAT-peptide is at least 10 000-fold less efficient than the toxin B-fragment (dtB) in mediating translocation of dtA to the cytosol.

It has been reported that heterologous proteins containing the TAT-peptide are more efficiently transported into the cell if they are first treated with 4 M urea, followed by rapid removal of the urea (*33*). The urea treatment is thought to induce a loose conformation of the proteins, thereby facilitating their transport across the lipid bilayer. Therefore, we treated TAT-dtA with 4 M urea, which was diluted 100-fold upon addition to the medium of cells, but we could still not detect any toxic effect (data not shown). The diphtheria toxin A-fragment is known to unfold at low pH, so we also tested the cytotoxicity of TAT-dtA that had been treated with pH 4.8, but no protein synthesis inhibition was observed (data not shown).

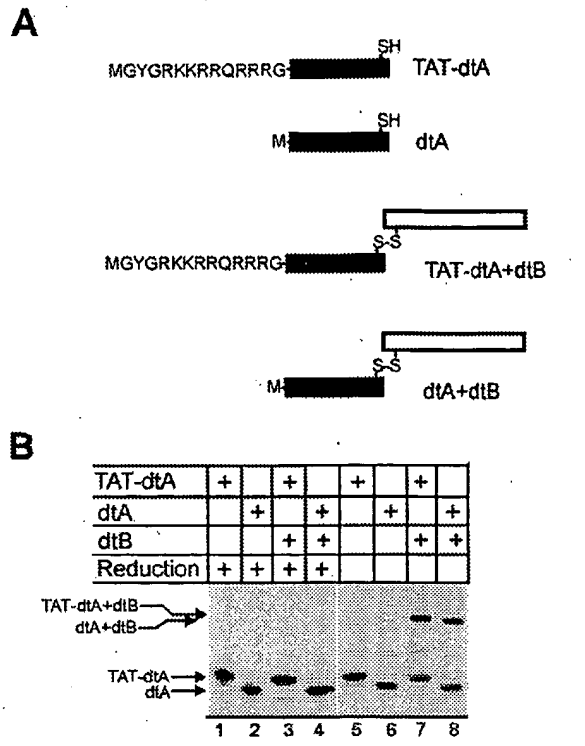

FIGURE 1: Description of constructs used and their in vitro translation products. (A) A filled box represents amino acids 2−189 of the diphtheria toxin A-fragment, i.e., the entire A-fragment except Gly1. dtA thus represents the wild-type A-fragment, except that Gly1 had been replaced by a methionine residue for the purpose of in vitro expression. An open box indicates the diphtheria toxin B-fragment. The sequence YGRKKRRQRRR is identical to residues 47−57 of the Tat protein. dtA and TAT-dtA can associate with the diphtheria toxin B-fragment, dtB, through disulfide bond formation, leading to the generation of the corresponding holotoxins, dtA+dtB and TAT-dtA+dtB, respectively. (B) Radiolabeled dtA and TAT-dtA were expressed by in vitro transcription followed by in vitro translation in a rabbit reticulocyte lysate in the presence of [^{35}S]methionine. Unlabeled dtB was expressed similarly, using unlabeled methionine instead of [^{35}S]methionine. The radiolabeled translation products, dtA and TAT-dtA, were dialyzed overnight against dialysis buffer, in some cases (lanes 3, 4, 7, 8) after mixing with translation mixture containing unlabeled B-fragment. The dialyzed translation mixtures were analyzed by reducing (lanes 1−4) or nonreducing (lanes 5−8) SDS−PAGE and fluorography.

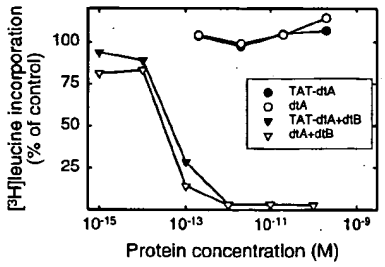

FIGURE 2: Cytotoxicity of reassociated holotoxins and free A-fragments. Vero cells were incubated overnight in the presence of unlabeled holotoxin or A-fragment. The cells were then incubated with [^{3}H]leucine, and cellular protein synthesis was measured by scintillation counting as the amount of radioactivity incorporated into TCA-precipitable material.

Translocation of TAT-dtA to the Cytosol by the Diphtheria Toxin Pathway. We could not exclude the possibility that the lack of toxicity of TAT-dtA was caused by a defect in its enzymatic activity rather than by an inability to enter the cytosol, and that the observed cytotoxic effect of the holotoxin, TAT-dtA+dtB, originated from toxin molecules where the TAT-peptide had been cleaved off during toxin entry. We therefore tested whether TAT-dtA is translocated to the cytosol by the diphtheria toxin pathway in its full-length form. When radiolabeled dtA+dtB is bound to cells, followed by a brief exposure of the cells to acidic pH, dtA is translocated to the cytosol (*14*, *15*). This can be detected as cell-mediated reduction of the interfragment disulfide bond (*34*), and the dtA generated by this process is protected against externally added Pronase (*35*). We performed an experiment where [^{35}S]methionine-labeled TAT-dtA+dtB (labeled only in TAT-dtA) was incubated with Vero cells at room temperature, followed by a brief exposure of the cells to a buffer of pH 7.0 or 4.8 at 37 °C. Subsequently, the cells were either lysed immediately or treated with Pronase to remove extracellular material before lysis. Finally, cellular proteins were precipitated with TCA, and analyzed by SDS−PAGE and fluorography. The results obtained with TAT-dtA+dtB (Figure 3, lanes 1−4) were similar to those obtained with the wild-type toxin dtA+dtB (Figure 3, lanes 5−8) in that exposure of the cells to pH 4.8 induced a reduction of the interfragment disulfide bond, and that the free A-fragment thus obtained was protected against externally added Pronase. Thus, the data indicate that TAT-dtA is translocated to the cytosol by the diphtheria toxin pathway in its full-length form. Interestingly, in these experiments we observed that although the amounts of toxin used were very similar, more TAT-dtA+dtB than dtA+dtB associated with the cells (Figure 3, compare lanes 1 and 5), and also, a substantial amount of free TAT-dtA was associated with the cells in the absence of exposure to low pH (Figure 3, lane 1).

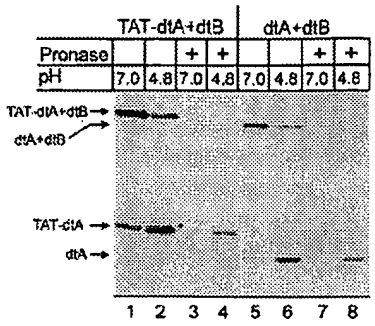

FIGURE 3: Translocation of TAT-dtA and dtA to the cytosol of Vero cells. Vero cells were incubated 20 min at 25 °C with translation mixture containing [^{35}S]methionine-labeled reassociated holotoxins (0.2 nM), and subsequently exposed for 5 min at 37 °C to MES−gluconate buffer of pH 7.0 (lanes 1, 3, 5, 7) or pH 4.8 (lanes 2, 4, 6, 8). The cells were then lysed in lysis buffer (lanes 1, 2, 5, 6) or treated with 5 mg/mL Pronase for 10 min at 37 °C before lysis was performed (lanes 3, 4, 7, 8). Nuclei were removed from the cell lysates by centrifugation, and proteins in the supernatant were precipitated with TCA and analyzed by nonreducing SDS−PAGE and fluorography.

Toxin Binding to Cells. The data in Figure 3 indicated that the attachment of the TAT-peptide to dtA leads to increased cellular association of both holotoxin and free A-fragment, and we decided to study this phenomenon in more detail. We incubated Vero cells at 4 °C with increasing concentrations of in vitro translated, [^{35}S]methionine-labeled toxin.

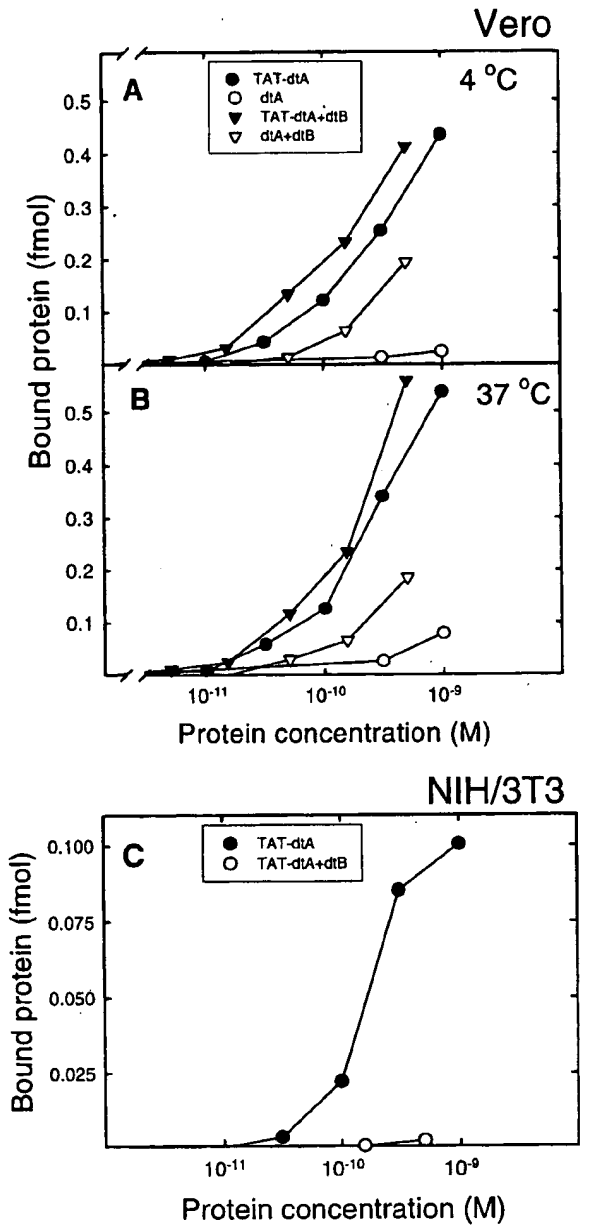

FIGURE 4: Binding of radiolabeled proteins to Vero (panels A and B) and NIH/3T3 (panel C) cells. The cells were incubated with increasing concentrations of translation mixture containing [^{35}S]-methionine-labeled holotoxin or free A-fragment for 1 h at 4 °C (panels A and C), or for 30 min at 37 °C (panel B). Unbound toxin was washed away, the cells were lysed in lysis buffer, and cellular proteins were precipitated with TCA and analyzed by nonreducing SDS−PAGE. The bands in the gels representing the various [^{35}S]-methionine-labeled proteins were quantitated by phosphorimaging (panels A and B) or by densitometric scanning of the film after fluorography (panel C).

Cell-associated proteins were subsequently analyzed by SDS−PAGE, and quantified by phosphorimaging. The results (Figure 4A) showed that while negligible amounts of free dtA associated with the cells, considerable binding of TAT-dtA was detected, actually more than in the case of wild-type holotoxin, dtA+dtB. Moreover, also the TAT-peptide-containing holotoxin, TAT-dtA+dtB, bound more efficiently than dtA+dtB to the cells. We also studied cellular association of the [^{35}S]methionine-labeled toxins at 37 °C, and the results (Figure 4B) were very similar to those obtained at 4 °C. Furthermore, we performed a binding experiment at 4 °C on mouse NIH/3T3 cells, which do not contain diphtheria toxin receptors (*36*). TAT-dtA bound to these cells (Figure 4C), but in less quantities than to Vero cells, possibly because Vero cells are very rich in surface heparans compared to other cell lines (*37*). We could only detect minute binding of TAT-dtA+dtB to the NIH/3T3 cells, presumably because the interaction between the TAT-peptide and the cell surface is weak, and thus capable of mediating binding of the relatively small TAT-dtA (23 kDa), but not that of the considerably larger TAT-dtA+dtB (60 kDa).

Interaction of TAT-dtA with Immobilized Heparin and Effects of Heparin on Binding to Cells. The Tat protein is, similarly to many other proteins, able to bind heparin (*24*), and the basic region which has been implicated in heparin binding (*23*) is contained within the TAT-peptide. We therefore suspected that the increased cell association conferred by the TAT-peptide may be due to the ability of this basic peptide to interact with heparin-like molecules on the cell surface.

We first tested the ability of TAT-dtA to adsorb to heparin−Sepharose in the presence of varying concentrations of NaCl. We found that TAT-dtA, but not dtA, bound to heparin−Sepharose at physiological salt concentrations (Figure 5A). The binding decreased as the NaCl concentration was increased, and the binding was reduced to 50% at 0.6 M NaCl (Figure 5A,C). For aFGF, a protein which is known to interact strongly with heparin (*38*), half-maximal binding was observed at 1 M NaCl (Figure 5B,C).

It was then investigated to what extent heparin and unlabeled diphtheria toxin interfered with cell binding of the toxins containing the TAT-peptide. The binding of both TAT-dtA and TAT-dtA+dtB to Vero cells was strongly reduced in the presence of heparin, while heparin had no effect on the binding of the wild-type toxin (Figure 5D), in accordance with previous studies (*37*). As expected, the binding of dtA+dtB to cells was diminished by the presence of unlabeled diphtheria toxin, while the binding of TAT-dtA was not affected. Also, most of the binding of TAT-dtA+dtB was abrogated by the presence of unlabeled diphtheria toxin. This observation, in combination with the low level of TAT-dtA+dtB binding to the receptor-less NIH/3T3 cells, suggests that although the TAT-peptide substantially increases the binding of the holotoxin to the cells, the majority of the toxin is actually bound to the diphtheria toxin receptor.

Potentiation of Toxic Effect of Diphtheria Toxin by the TAT-Peptide. An apparent discrepancy exists between the toxicity (Figure 2) and binding and translocation experiments performed with TAT-dtA+dtB, in that this protein showed increased association with cells relative to dtA+dtB, while the toxicity of these two proteins was basically equal. The binding and toxicity experiments differed in that binding was measured as the amount of radiolabeled protein associated with the cells during a 30−60 min period, while the toxicity was measured after an overnight incubation with toxin, thus allowing several rounds of toxin binding and internalization. Therefore, we also performed experiments where the toxicity was measured after a relatively short binding period.

In the first experiment, toxin was bound to Vero cells for 1 h at 4 °C, unbound toxin washed away, and the translo-

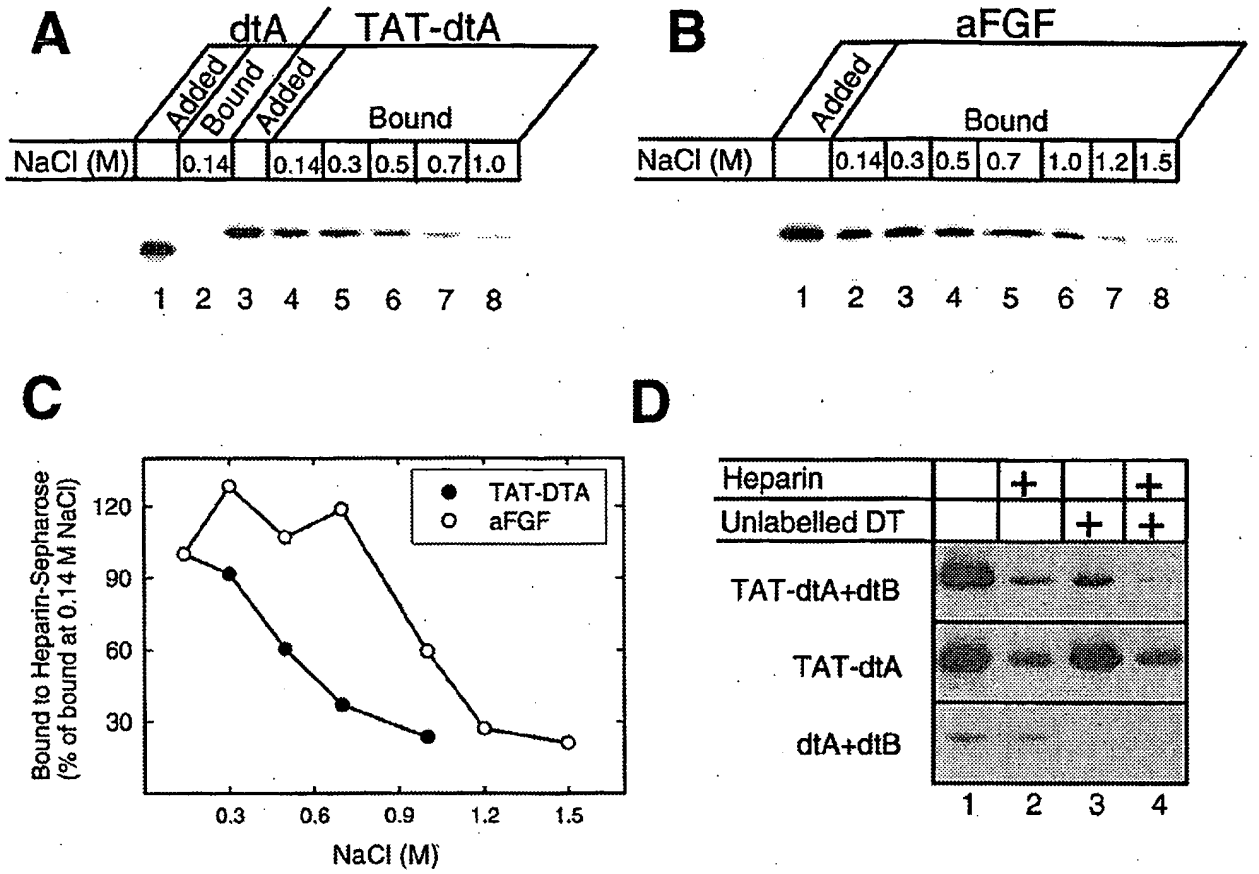

FIGURE 5: Interaction of TAT-dtA with heparin and effect of heparin on toxin binding to cells. (A) An aliquot of translation mixture containing [^{35}S]methionine-labeled dtA or TAT-dtA was adsorbed to heparin−Sepharose for 1 h at 4 °C in PBS containing the indicated concentrations of NaCl. The adsorbed material was eluted with SDS−PAGE sample buffer and analyzed by reducing SDS−PAGE and fluorography. In some cases (lanes 1 and 3), the aliquot was subjected directly to SDS−PAGE, without any adsorption to heparin−Sepharose. (B) Same as panel A, but translation mixture containing [^{35}S]methionine-labeled aFGF was used. (C) The bands in the gels in panels A and B were quantitated by phosphorimaging, and the amount of adsorbed material was plotted as a function of NaCl concentration. (D) [^{35}S]Methionine-labeled proteins (0.1 nM) were bound to Vero cells for 1 h at 4 °C in an experiment similar to that described in Figure 4. When indicated, heparin (15 units/mL), unlabeled diphtheria toxin (50 μg/mL), or a combination of the two was present during binding.

cation of the A-fragment to the cytosol induced by exposure to low pH. Subsequently, translocated toxin was allowed to express its effect during an overnight incubation in the absence of exogenous toxin, before cellular protein synthesis was measured. In this experiment (Figure 6A), TAT-dtA+dtB displayed increased toxicity relative to dtA+dtB, and this increase was abolished when heparin was present during the incubation with toxin. On the other hand, heparin had no effect on the toxicity of the wild-type toxin, dtA+dtB.

We wanted to test whether the potentiation of the toxicity of diphtheria toxin by the TAT-peptide could be observed also when the toxin entered the cells by its normal mechanism, i.e., endocytosis. Thus, Vero cells were incubated 30 min at 37 °C with toxin, washed, and subsequently incubated overnight in the absence of toxin before cellular protein synthesis was measured. The results (Figure 6B) were virtually identical to those obtained when the toxin was bound at 4 °C and toxin translocation induced by low pH; i.e., the TAT-peptide caused increased toxic effect, and this increase was abolished by the presence of heparin during the incubation with toxin.

Characterization of a Fusion Protein between VP22 and dtA. The Herpes simplex virus type 1 protein VP22 has been reported to translocate into neighboring cells when overexpressed in one cell, and also to enter cells when added externally (*4*). Furthermore, it has been reported that fused passenger proteins are translocated into cells along with VP22, and it has been suggested that VP22 can be used as a general vehicle to transport proteins into cells (*4*).

To test the efficiency of VP22 transport into cells, we fused dtA to VP22 (Figure 7A), and the resulting heterologous protein was expressed in a rabbit reticulocyte lysate. We then tested the toxicity of the fusion protein VP22-dtA in Vero cells. Surprisingly, we did not detect any toxicity of VP22-dtA in the concentration range tested, while the diphtheria holotoxin (dtA + dtB) was very toxic to the cells (Figure 7B). In contrast to the holotoxin containing the TAT-peptide, TAT-dtA+dtB, the holotoxin VP22-dtA+dtB was not able to translocate efficiently into cells by the diphtheria toxin pathway, as indicated from toxicity and Pronase protection assays (data not shown). Conceivably, the reason for the lack of VP22-dtA cytotoxicity could be due to impairment of the enzymatic activity of dtA when fused to VP22. We therefore analyzed the activity of VP22-dtA by an in vitro assay to test its ADP-ribosylating ability. We found that VP22-dtA only displayed moderate reduction in

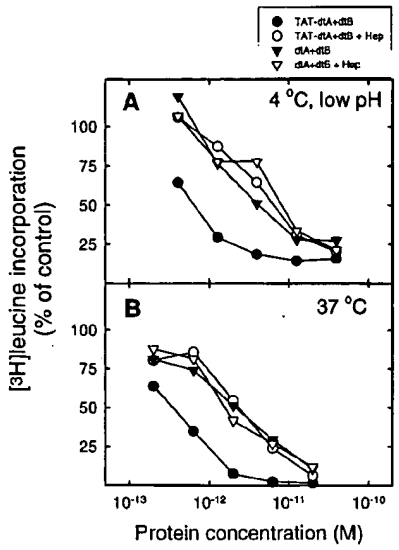

FIGURE 6: Increased toxicity of TAT-dtA upon short-term exposure to toxin and inhibition by heparin. (A) Increasing concentrations of reassociated holotoxin were incubated with Vero cells for 1 h at 4 °C, when indicated (open symbols) in the presence of heparin (15 units/mL). The cells were then exposed to MES−gluconate buffer, pH 4.8, for 5 min at 37 °C, and subsequently incubated overnight in growth medium, before cellular protein synthesis was measured as outlined in Figure 2. (B) Same as in panel A, except that the cells were incubated 30 min at 37 °C with toxin, and then incubated overnight in growth medium.

enzymatic activity (~50%) compared to dtA alone (data not shown), indicating that upon translocation to the cytosol, VP22-dtA should be able to inhibit cellular protein synthesis rather efficiently.

In analogy to the TAT-peptide, VP22 can bind to polyanions and heparin (*26*), and we therefore tested if VP22-dtA could bind to immobilized heparin. As seen in Figure 7C, this fusion protein binds to heparin−Sepharose, while dtA does not. We also tested if [^{35}S]methionine-labeled VP22-dtA binds to Vero cells. The results (Figure 7D) showed that this protein associated with the cells, and the binding was competed out by heparin. Taken together, our results suggest that VP22-dtA is not able to translocate into cells, at least in the concentration range tested here, even if this fusion protein binds to cells.

DISCUSSION

In the present work, we have demonstrated that the attachment of a short basic region from the TAT protein converts dtA into a heparin-binding protein, which also displays substantial binding to cells. The TAT-peptide also conferred increased binding and toxicity to the holotoxin, and the effects of the fused TAT-peptide could be reverted through the addition of exogenous heparin. Although the TAT-peptide has been reported to mediate transport of a number of proteins into cells, we could not detect any cytotoxicity of TAT-dtA. Similar results were obtained in the case of a fusion between the viral protein VP22 and dtA.

It was discovered in 1988 that exogenous Tat enters cells, leading to trans-activation (*5*, *6*), and the cellular uptake of Tat protein has later been extensively studied. There are a high number (>10^7) of low-affinity binding sites for Tat at the cell surface, and binding and trans-activation can be inhibited by the addition of polyanions such as dextran sulfate and heparin (*39*). Accordingly, Tat has been reported to bind immobilized heparin through its polybasic region (*23*, *24*), which has also been implicated in binding to cells (*39*), thus indicating that Tat can bind to cell-surface heparans. However, Tat appears to bind to cells by several different mechanisms, since it also can interact with cell-surface integrins, both through its polybasic domain (*40*) and through its integrin-binding motif, an RGD sequence (*41*, *42*). Surface-bound Tat is internalized, and this process is blocked at 4 °C, at least in some cell types (*39*), suggesting that conventional endocytosis occurs.

TAT-dtA behaves similarly to Tat in that it binds heparin, and that it displays cell binding which can be competed out by exogenously added heparin. With the modest amounts of toxin expressed in the reticulocyte lysates, we could not saturate the binding sites, and thus calculate neither the affinity nor the number of binding sites. However, we believe that TAT-dtA, similarly to TAT, binds to abundant, low-affinity binding sites on cells. In NIH/3T3 cells, that lack the toxin receptor, we could detect substantial binding of the holotoxin TAT-dtA (22 kDa), but only minute binding of the larger (60 kDa) holotoxin TAT-dtA+dtB, thus indicating that the interaction between the TAT-peptide and surface heparans may be rather weak. In accordance with this, most of the binding of the holotoxin TAT-dtA+dtB to Vero cells, that have toxin receptors, could be competed out by unlabeled diphtheria toxin. Also, the increased binding of TAT-dtA+dtB to Vero cells was accompanied by a comparable increase in short-term cytotoxicity. Since an intact toxin receptor, and not simply binding of the toxin to the cell surface, is required for efficient intoxication (*43*−*45*), we favor a model where the majority of the bound TAT-dtA+dtB molecules are associated with the toxin receptor, and where binding of the TAT-peptide to the cell surface, possibly via heparans, enhances binding to the toxin receptor. It may appear enigmatic that an added TAT-peptide was able to potentiate the toxic effect of diphtheria toxin when the cells where exposed shortly to the toxin, but not when the toxin was present during an overnight incubation. However, considerably less (~10 times) toxin was required to inhibit protein synthesis in the overnight experiment relative to the short-term experiment, and it is likely that the low-affinity interaction between the TAT-peptide and surface molecules is less capable of enhancing binding to the toxin receptor at low concentrations.

During the last years, several peptide sequences have been reported to be able to penetrate cellular membranes when added extracellularly, and thus be able to deliver cargo, such as peptides and nucleic acids, into the cells (reviewed in refs *19*, *22*, *46*, *47*). The entry of such peptides has usually been studied by immunofluorescence microscopy or by assaying for the biological activity of a cargo molecule, and virtually nothing is known with respect to the entry mechanism and by which efficiency they reach the target site (typically the cytosol or the nucleus). When biological effects of proteins or peptides fused to these membrane-permeable sequences have been studied, rather high protein concentrations (10^{-7}−10^{-4} M) have been applied to the cells. On the other hand, protein toxins have also been used to transport biologically active molecules into cells, and effects can be observed at

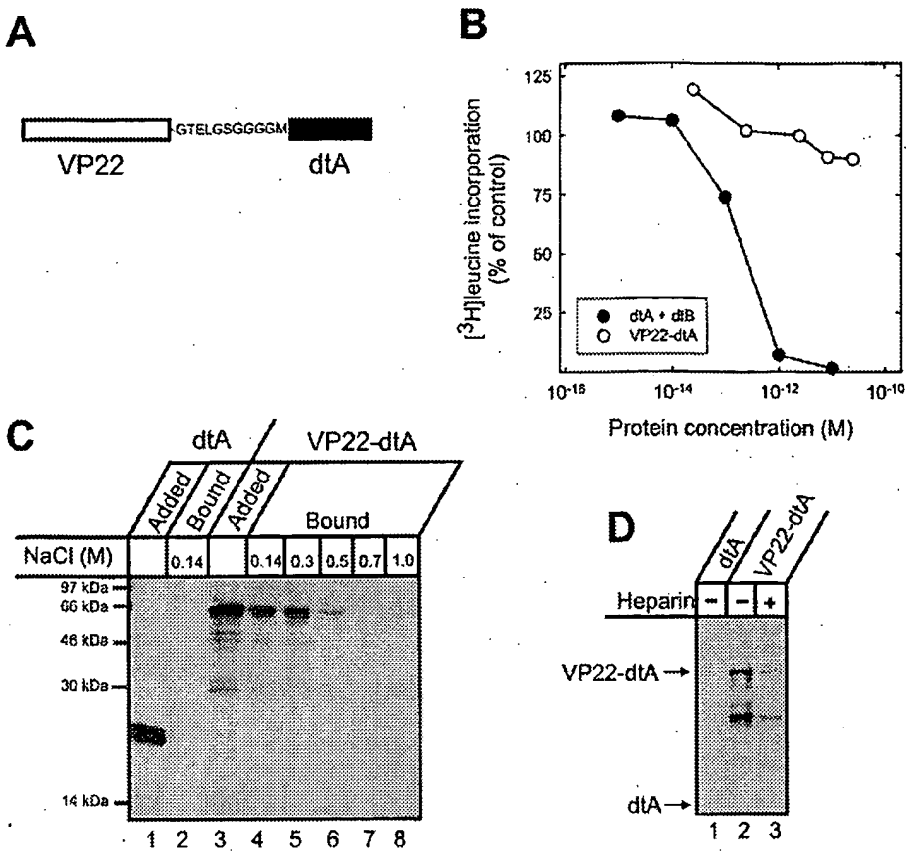

FIGURE 7: Characterization of VP22-dtA. (A) Schematic presentation of VP22-dtA. A glycine-rich linker was inserted between the two proteins to provide flexibility and facilitate correct folding. (B) Toxicity experiment as described in Figure 2 was performed. VP22-dtA, open circles; dtA+dtB, closed circles. (C) Adsorption of VP22-dtA to heparin−Sepharose in the presence of increasing concentrations of NaCl was performed as described in Figure 5. (D) Binding of VP22-dtA to Vero cells. The experiment was performed as described in Figure 4. When indicated, 15 units/mL heparin was present during binding.

much lower concentrations (10^{-11}−10^{-10} M) (*36*, *48*). This suggests that these membrane-permeable sequences may actually be rather inefficient in delivering cargo to the cytosol. In the present study, we have used in vitro translation in a reticulocyte lysate for protein expression. We have therefore only obtained small quantities of protein, and in the toxicity experiments we have not been able to use higher protein concentrations than 5×10^{-10} M. For better comparison with previous studies on proteins containing membrane-permeant sequences, it would definitely have been favorable being able to use higher protein concentrations, and through expression in *E. coli*, we would most likely have been able to obtain larger amounts of protein. However, it is generally considered dangerous to clone and express full-length protein toxins in *E. coli*, and we reasoned that *E. coli* overexpressing dtA fused to a membrane-permeable sequence may represent a biohazard, and we therefore chose the in vitro translation system for expression.

dtA is able to translocate efficiently to the cytosol in the context of the holotoxin, and one molecule of dtA in the cytosol is sufficient to kill a cell. We therefore chose to use dtA as a model protein for evaluating the efficiency of transport to the cytosol mediated by the TAT-peptide and VP22. Peptides fused to the N-terminal end of dtA can be efficiently translocated to the cytosol in the context of the holotoxin, while C-terminal extensions tend to block translocation or toxin binding to cells (*49*). We therefore chose to fuse the TAT-peptide and VP22 to the N-terminus of dtA. Although we observed substantial binding of TAT-dtA and VP22-dtA to cells, we could not detect any cytotoxicity. Specifically, in the case of TAT-dtA, substantially more binding to cells was observed than in the case of the wild-type toxin, but still no cytotoxicity was detected, indicating that the TAT-peptide is at least 4 orders of magnitude less efficient than dtB in translocating dtA to the cytosol. Our data therefore indicate that both the TAT-peptide and VP22 are inefficient at delivering dtA to the cytosol.

Even with the low concentrations used in our experiments (<1 nM), we detected substantial binding of TAT-dtA to cells. When the TAT-peptide has been used to transport biologically active molecules into cells, considerably higher concentrations (typically 100 nM) have been used. It is therefore likely that a high number of molecules are bound to each cell, but that the observed biological effects are provided by a small subpopulation of molecules that have reached the desired destination (the cytosol or the nucleus). Consequently, when immunofluorescence is used to evaluate the ability of such proteins to translocate into cells, caution should be taken, since the majority of the detected fluorescence may originate from molecules that have not reached the desired destination. Also, three independent reports indicate that some of the apparent membrane translocating

properties of VP22 observed in fluorescence studies may be caused by artifacts caused by the fixation procedure used (*50*−*52*). It would definitely have been interesting to study the fluorescence patterns obtained with VP22-dtA and TAT-dtA and compare them with those obtained with the TAT-dtA+dtB holotoxin, or with TAT or VP22 fusion proteins that have previously been detected intracellularly by immunofluorescence. However, with the rather small amounts of protein obtained from the reticulocyte lysate, we expect it to be very difficult to detect cell-associated TAT-dtA or VP22-dtA by immunofluorescence.

It is an intriguing concept that some peptide sequences could readily penetrate lipid bilayers, and, moreover, be able to carry cargo across the membrane. However, since relatively high concentrations are required to observe biological effects, it has in our view not yet been established that these peptides are *efficient* vehicles for intracellular delivery of macromolecules, or if they have any intrinsic membrane penetrating activity. An alternative explanation is that these peptides provide massive association with the cell surface, possibly through interaction with cell-surface heparans, and that a very small fraction of the cell-associated molecules are able to reach the desired destination where a biological effect is exerted. Ligands that bind to cell-surface heparans are endocytosed (reviewed in ref *53*), and a minute fraction of the endocytosed molecules may be able to escape to the cytosol from intracellular organelles upon endocytosis.

Evidence is accumulating that some protein toxins, e.g., ricin and Shiga toxin, upon endocytosis traverse the secretory pathway in the opposite direction, and finally translocate to the cytosol through the ER membrane (*54*, *55*). Ricin is toxic at concentrations as low as 10^{-11}−10^{-10} M, while free ricin A-chain taken up by fluid-phase endocytosis displays toxicity at concentrations around 10^{-6} M. The fusion of an ER retrieval signal, i.e., a KDEL sequence, to the free ricin A-chain increased its toxicity (*56*), indicating that transport to the ER is important for translocation to the cytosol. Also, when receptor-binding ligands were fused to the ricin A-chain, highly potent toxins were obtained (toxic at 10^{-9} M) (*57*−*59*). The isolated diphtheria toxin A-fragment is nontoxic, but when linked to receptor-binding peptide hormones such as insulin or chorionic gonadotropin, the resulting heterologous proteins were moderately toxic (at 10^{-7} M) toward cells carrying the corresponding hormone receptors (*60*, *61*). Gelonin is a plant protein which inhibits cellular protein synthesis by the same mechanism as the ricin A-chain, but it does not contain a receptor-binding domain, and therefore displays low cytotoxicity. However, its toxicity was potentiated through conjugation with galactose- and mannose-terminating glycoproteins (*62*), or with the lectin concanavalin A (*63*), thereby allowing binding to receptors at the cell surface. Thus, an important lesson to be learned from the toxin field is that several different receptor-binding ligands can form highly toxic proteins when fused to protein synthesis inhibitors devoid of any membrane translocating activity. Our results indicate that both the TAT-peptide and VP22 can confer association of heterologous proteins with cells. In our view, the possibility should be kept in mind that the apparent membrane penetrating abilities of these proteins really may reflect their ability to associate with the cell surface.

ACKNOWLEDGMENT

We are grateful to Frøydis Kristoffersen and Sissel Håvåg for their expert handling of the cell cultures, and to Dr. Olav Klingenberg for critical reading of the manuscript.

REFERENCES

1. Falnes, P. O., and Sandvig, K. (2000) *Curr. Opin. Cell Biol. 12*, 407.
2. Jans, D. A., and Hassan, G. (1998) *Bioessays 20*, 400.
3. Prochiantz, A. (2000) *Curr. Opin. Cell Biol. 12*, 400.
4. Elliott, G., and O'Hare, P. (1997) *Cell 88*, 223.
5. Frankel, A. D., and Pabo, C. O. (1988) *Cell 55*, 1189.
6. Green, M., and Loewenstein, P. M. (1988) *Cell 55*, 1179.
7. Greenfield, L., Bjorn, M. J., Horn, G., Fong, D., Buck, G. A., Collier, R. J., and Kaplan, D. A. (1983) *Proc. Natl. Acad. Sci. U.S.A. 80*, 6853.
8. Drazin, R., Kandel, J., and Collier, R. J. (1971) *J. Biol. Chem. 246*, 1504.
9. Collier, R. J., and Kandel, J. (1971) *J. Biol. Chem. 246*, 1496.
10. Uchida, T., Pappenheimer, A. M., Jr., and Harper, A. A. (1972) *Science 175*, 901.
11. Naglich, J. G., Metherall, J. E., Russell, D. W., and Eidels, L. (1992) *Cell 69*, 1051.
12. Blewitt, M. G., Chung, L. A., and London, E. (1985) *Biochemistry 24*, 5458.
13. Dumont, M. E., and Richards, F. M. (1988) *J. Biol. Chem. 263*, 2087.
14. Draper, R. K., and Simon, M. I. (1980) *J. Cell Biol. 87*, 849.
15. Sandvig, K., and Olsnes, S. (1980) *J. Cell Biol. 87*, 828.
16. Falnes, P. O., and Olsnes, S. (1995) *J. Biol. Chem. 270*, 20787.
17. Falnes, P. O., Ariansen, S., Sandvig, K., and Olsnes, S. (2000) *J. Biol. Chem. 275*, 4363.
18. Yamaizumi, M., Mekada, E., Uchida, T., and Okada, Y. (1978) *Cell 15*, 245.
19. Schwarze, S. R., Hruska, K. A., and Dowdy, S. F. (2000) *Trends Cell Biol. 10*, 290.
20. Fawell, S., Seery, J., Daikh, Y., Moore, C., Chen, L. L., Pepinsky, B., and Barsoum, J. (1994) *Proc. Natl. Acad. Sci. U.S.A. 91*, 664.
21. Phelan, A., Elliott, G., and O'Hare, P. (1998) *Nat. Biotechnol. 16*, 440.
22. Derossi, D., Chassaing, G., and Prochiantz, A. (1998) *Trends Cell Biol. 8*, 84.
23. Rusnati, M., Tulipano, G., Urbinati, C., Tanghetti, E., Giuliani, R., Giacca, M., Ciomei, M., Corallini, A., and Presta, M. (1998) *J. Biol. Chem. 273*, 16027.
24. Albini, A., Benelli, R., Presta, M., Rusnati, M., Ziche, M., Rubartelli, A., Paglialunga, G., Bussolino, F., and Noonan, D. (1996) *Oncogene 12*, 289.
25. Farahbakhsh, Z. T., Baldwin, R. L., and Wisnieski, B. J. (1987) *J. Biol. Chem. 262*, 2256.
26. Kueltzo, L. A., O'Hare, P., and Middaugh, C. R. (2000) *J. Biol. Chem.* (in press).
27. Sandvig, K., and Olsnes, S. (1981) *J. Biol. Chem. 256*, 9068.
28. Ariansen, S., Afanasiev, B. N., Moskaug, J. O., Stenmark, H., Madshus, I. H., and Olsnes, S. (1993) *Biochemistry 32*, 83.
29. McGill, S., Stenmark, H., Sandvig, K., and Olsnes, S. (1989) *EMBO J. 8*, 2843.
30. Stenmark, H., Afanasiev, B. N., Ariansen, S., and Olsnes, S. (1992) *Biochem. J. 281*, 619.
31. Falnes, P. O., Choe, S., Madshus, I. H., Wilson, B. A., and Olsnes, S. (1994) *J. Biol. Chem. 269*, 8402.
32. Vocero-Akbani, A. M., Heyden, N. V., Lissy, N. A., Ratner, L., and Dowdy, S. F. (1999) *Nat. Med. 5*, 29.
33. Nagahara, H., Vocero-Akbani, A. M., Snyder, E. L., Ho, A., Latham, D. G., Lissy, N. A., Becker-Hapak, M., Ezhevsky, S. A., and Dowdy, S. F. (1998) *Nat. Med. 4*, 1449.
34. Moskaug, J. O., Sandvig, K., and Olsnes, S. (1987) *J. Biol. Chem. 262*, 10339.
35. Moskaug, J. O., Sandvig, K., and Olsnes, S. (1988) *J. Biol. Chem. 263*, 2518.

36. Wiedlocha, A., Falnes, P. O., Madshus, I. H., Sandvig, K., and Olsnes, S. (1994) *Cell 76*, 1039.
37. Shishido, Y., Sharma, K. D., Higashiyama, S., Klagsbrun, M., and Mekada, E. (1995) *J. Biol. Chem. 270*, 29578.
38. Maciag, T., Mehlman, T., Friesel, R., and Schreiber, A. B. (1984) *Science 225*, 932.
39. Mann, D. A., and Frankel, A. D. (1991) *EMBO J. 10*, 1733.
40. Vogel, B. E., Lee, S. J., Hildebrand, A., Craig, W., Pierschbacher, M. D., Wong-Staal, F., and Ruoslahti, E. (1993) *J. Cell Biol. 121*, 461.
41. Brake, D. A., Debouck, C., and Biesecker, G. (1990) *J. Cell Biol. 111*, 1275.
42. Barillari, G., Sgadari, C., Fiorelli, V., Samaniego, F., Colombini, S., Manzari, V., Modesti, A., Nair, B. C., Cafaro, A., Sturzl, M., and Ensoli, B. (1999) *Blood 94*, 663.
43. Almond, B. D., and Eidels, L. (1994) *J. Biol. Chem. 269*, 26635.
44. Lanzrein, M., Sand, O., and Olsnes, S. (1996) *EMBO J. 15*, 725.
45. Stenmark, H., Olsnes, S., and Sandvig, K. (1988) *J. Biol. Chem. 263*, 13449.
46. Lindgren, M., Hallbrink, M., Prochiantz, A., and Langel, U. (2000) *Trends Pharmacol. Sci. 21*, 99.
47. Hawiger, J. (1999) *Curr. Opin. Chem. Biol. 3*, 89.
48. Arora, N., and Leppla, S. H. (1994) *Infect. Immun. 62*, 4955.
49. Stenmark, H., Moskaug, J. O., Madshus, I. H., Sandvig, K., and Olsnes, S. (1991) *J. Cell Biol. 113*, 1025.
50. Pomeranz, L. E., and Blaho, J. A. (1999) *J. Virol. 73*, 6769.
51. Fang, B., Xu, B., Koch, P., and Roth, J. A. (1998) *Gene Ther. 5*, 1420.
52. Aints, A., Dilber, M. S., and Smith, C. I. (1999) *J. Gene Med. 1*, 275.
53. Williams, K. J., and Fuki, I. V. (1997) *Curr. Opin. Lipidol. 8*, 253.
54. Hazes, B., and Read, R. J. (1997) *Biochemistry 36*, 11051.
55. Rapak, A., Falnes, P. O., and Olsnes, S. (1997) *Proc. Natl. Acad. Sci. U.S.A. 94*, 3783.
56. Wales, R., Roberts, L. M., and Lord, J. M. (1993) *J. Biol. Chem. 268*, 23986.
57. Cawley, D. B., Herschman, H. R., Gilliland, D. G., and Collier, R. J. (1980) *Cell 22*, 563.
58. Till, M. A., Ghetie, V., Gregory, T., Patzer, E. J., Porter, J. P., Uhr, J. W., Capon, D. J., and Vitetta, E. S. (1988) *Science 242*, 1166.
59. Sundan, A., Olsnes, S., Sandvig, K., and Pihl, A. (1982) *J. Biol. Chem. 257*, 9733.
60. Oeltmann, T. N. (1985) *Biochem. Biophys. Res. Commun. 133*, 430.
61. Miskimins, W. K., and Shimizu, N. (1979) *Biochem. Biophys. Res. Commun. 91*, 143.
62. Stockert, R. J., Potvin, B., Tao, L., Stanley, P., and Wolkoff, A. W. (1995) *J. Biol. Chem. 270*, 16107.
63. Stirpe, F., Olsnes, S., and Pihl, A. (1980) *J. Biol. Chem. 255*, 6947.

BI002443L

STIC-ILL

From: Canella, Karen
Sent: Thursday, May 22, 2003 9:50 PM
To: STIC-ILL
Subject: ill order 10/033,577

Art Unit 1642 Location 8E12(mail)

Telephone Number 308-8362

Application Number 10/033,577

1. Biochemistry, 2001 Apr 10, 40(4):4349-4358

2. PNAS, 1982, 79(9):2912-2916

3. Protein engineering, 1995, Vol. 8, suppl., page 123.

Targeting of Pseudomonas and Diphtheria toxins to the α2-macroglobulin receptor via RAP-toxin and PAI-1-toxin fusions.

Alexey G. Zdanovsky+, Marina V. Zdanovskaia+, Dudley Strickland@, and David J. FitzGerald+.

+From the Laboratory of Molecular Biology, National Cancer Institute, Division of Cancer Biology, Diagnosis and Centres, National Institutes of Health, Bethesda, MD 20892.
@From the Biochemistry Laboratory, American Red Cross, Rockville, MD 20855.

INTRODUCTION

The α2-macroglobulin receptor/low density lipoprotein receptor-related protein (α2MR/LRP) has been shown to mediate the binding and endocytosis of several unrelated ligands. Among them, are lipoprotein lipase, α2-macroglobulin-protease complexes and tissue-type plasminogen activator (tPA)-plasminogen activator inhibitor type 1(PAI-1) complexes. A 39-kDa receptor-associated protein, called RAP, also binds to α2MR/LRP. RAP inhibits the binding of all known ligands to α2MR/LRP. In addition *Pseudomonas aeruginosa* exotoxin A (ETA) binds the heavy chain of α2MR/LRP and uses this interaction to gain entry to cells. ETA and a similar bacterial toxin, diphtheria toxin (DT), are toxic for cells because they inactivate the protein synthetic apparatus of eukaryotic cells. For both ETA and DT, a catalytically active fragment has to be generated which then translocates to the cytosol and ADP-ribosylates elongation factor 2 (EF-2).

In the present study we have attempted to determine whether or not different ligands that bind α2MR/LRP follow the same internal pathway after endocytosis.

RESULTS AND DISCUSSION.

We have constructed RAP-toxin derivatives whereby RAP replaced the binding domains of DT and ETA. These hybrids, DT-RAP and RAP-ETA, as well as native RAP exhibited heparin-binding activity. In addition the RAP-toxins bound to immobilized α2MR/LRP and this binding was inhibited by addition of heparin.

RAP-ETA and DT-RAP were less toxic for cells than unmodified ETA. This was seen despite the fact that the RAP-toxins bound to the α2MR/LRP with higher apparent affinity than ETA. Also, the complex between RAP-ETA and α2MR/LRP was stable at low pH. Therefore, we speculate that the RAP-toxins, entering the cell via α2MR/LRP, may not dissociate from the receptor and because of this are directed along a different intracellular pathway from native ETA.

Previously, we described a competition assay which defined a novel rate-limiting step in the ETA pathway (1). In this assay, enzymatically inactive ETA competed for the toxic effects of the native toxin. Competition required the presence of tryptophan at residue 281. An ETA mutant, with alanine in place of tryptophan 281 failed to compete for toxicity. We have produced a similar mutation in the RAP-ETA construct. Results showed that RAP-ETA with alanine at 281 was less able to compete for toxicity than RAP-ETA. Therefore, we conclude that at least some portion of RAP-ETA follows the same pathway as native toxin. This means that inside cells, the RAP-toxins are transported along a minimum of two pathways. However, the pathway that results in translocation to the cytosol appears not to be the primary one.

To examine the ability of another ligand to internalize one of these toxins, a fusion protein between DT and PAI-1 was made. The hybrid protein, DT-PAI-1, was able to interact with tPA. To show this, we demonstrated that interaction of the PAI-1 with tPA results in a complex that is stable even in the presence of SDS. We also noted that the incubation of tPA with our hybrid protein resulted in the inhibition of proteinase activity as measured by ability of tPA to cleave N-methylsulfonyl-D-Phe-Gly-Arg-4-nitranilide acetate.

The tPA-DT-PAI-1 complex was about 16 times more toxic for Cos cells than DT-PAI-1 alone, nevertheless it was about 4000 times less toxic than ETA and about 20,000 times less toxic than DT. The ID_{50} for this complex was 15 nM. At the same time ID_{50} for RAP-ETA and DT-RAP were 1.8 nM and 0.8 nM, respectively.

CONCLUSION

The α2MR/LRP transfers bound ligands to lysosomes where they are degraded. Possibly, only ligands that can dissociate from the α2MR/LRP, prior to reaching the lysosome, are able to follow a pathway that allows the transport of the catalytic domain to the cytosol. In this case, we speculate that the higher the affinity of the ligand for the α2MR/LRP the lower the chances that the catalytic domain will reach the cytosol.

REFERENCES

1. Zdanovsky, A.G., Chiron, M., Pastan, I., and FitzGerald, D.J. (1993) *J. Biol. Chem.* 268, 21791-21799.